Exploring the phase structure of the multi-flavor Schwinger model with quantum computing

Stefan Kühn
Computation-based Science and Technology Research Center, The Cyprus Institute

in collaboration with

Lena Funcke	MIT
Tobias Hartung	University of Bath
Karl Jansen	DESY Zeuthen
Marc-Oliver Pleinert	FAU Erlangen-Nürnberg
Stephan Schuster	FAU Erlangen-Nürnberg
Joachim von Zanthier	FAU Erlangen-Nürnberg

Lattice 2022

1. Multi-flavor Schwinger model on the lattice
2. Variational Quantum Eigensolver
3. Preliminary results
4. Summary & Outlook

Multi-flavor Schwinger model

Lattice multi-flavor Schwinger model

- Lattice formulation with Kogut-Susskind staggered fermions

$$H = -\frac{i}{2a}\sum_{n=1}^{N-1}\sum_{f=1}^{F}\left(\phi_{n,f}^{\dagger}\, e^{i\theta_n}\, \phi_{n+1,f} - \mathrm{h.c}\right) + \sum_{n=1}^{N}\sum_{f=1}^{F}\left((-1)^n m_f + \kappa_f\right)\phi_{n,f}^{\dagger}\phi_{n,f} + \frac{ag^2}{2}\sum_{n=1}^{N-1} L_n^2$$

Multi-flavor Schwinger model

Lattice multi-flavor Schwinger model

- Lattice formulation with Kogut-Susskind staggered fermions

$$H = -\frac{i}{2a}\sum_{n=1}^{N-1}\sum_{f=1}^{F}\left(\phi^{\dagger}_{n,f}\, e^{i\theta_n}\, \phi_{n+1,f} - \mathrm{h.c}\right) + \sum_{n=1}^{N}\sum_{f=1}^{F}\left((-1)^n m_f + \kappa_f\right)\phi^{\dagger}_{n,f}\phi_{n,f} + \frac{ag^2}{2}\sum_{n=1}^{N-1} L_n^2$$

Kinetic part + Coupling to gauge field   Mass term   Chemical potential   Electric energy

Multi-flavor Schwinger model

Lattice multi-flavor Schwinger model

- Lattice formulation with Kogut-Susskind staggered fermions

$$H = -\frac{i}{2a}\sum_{n=1}^{N-1}\sum_{f=1}^{F}\left(\phi^{\dagger}_{n,f}\, e^{i\theta_n}\, \phi_{n+1,f} - \text{h.c}\right) + \sum_{n=1}^{N}\sum_{f=1}^{F}\left(\boxed{(-1)^n m_f} + \boxed{\kappa_f}\right)\phi^{\dagger}_{n,f}\phi_{n,f} + \frac{ag^2}{2}\sum_{n=1}^{N-1}\boxed{L_n^2}$$

Kinetic part + Coupling to gauge field Mass term Chemical potential Electric energy

- Gauss Law: $L_n - L_{n-1} = Q_n = \sum_{f=1}^{F}\left[\phi^{\dagger}_{n,f}\phi_{n,f} - \frac{1}{2}\left(1-(-1)^n\right)\right]$

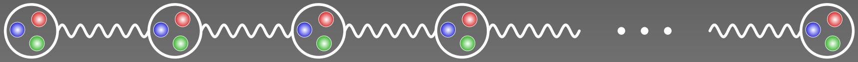

Multi-flavor Schwinger model

Lattice multi-flavor Schwinger model

- Lattice formulation with Kogut-Susskind staggered fermions

$$H = -\frac{i}{2a}\sum_{n=1}^{N-1}\sum_{f=1}^{F}\left(\phi^{\dagger}_{n,f}\, e^{i\theta_n}\, \phi_{n+1,f} - \text{h.c}\right) + \sum_{n=1}^{N}\sum_{f=1}^{F}\left((-1)^n m_f + \kappa_f\right)\phi^{\dagger}_{n,f}\phi_{n,f} + \frac{ag^2}{2}\sum_{n=1}^{N-1} L_n^2$$

Kinetic part + Coupling to gauge field

Mass term

Chemical potential

Electric energy

- Gauss Law: $L_n - L_{n-1} = Q_n = \sum_{f=1}^{F}\left[\phi^{\dagger}_{n,f}\phi_{n,f} - \frac{1}{2}\left(1-(-1)^n\right)\right]$
- Use open boundary conditions and Gauss Law to integrate out the gauge field

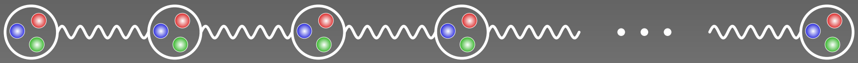

$l_0 + Q_1 = l_1$

Multi-flavor Schwinger model

Lattice multi-flavor Schwinger model

- Lattice formulation with Kogut-Susskind staggered fermions

$$H = \underbrace{-\frac{i}{2a}\sum_{n=1}^{N-1}\sum_{f=1}^{F}\left(\phi^\dagger_{n,f}\, e^{i\theta_n}\, \phi_{n+1,f} - \text{h.c}\right)}_{\text{Kinetic part + Coupling to gauge field}}$$

$$+\sum_{n=1}^{N}\sum_{f=1}^{F}\Big(\underbrace{(-1)^n m_f}_{\text{Mass term}} + \underbrace{\kappa_f}_{\text{Chemical potential}}\Big)\phi^\dagger_{n,f}\phi_{n,f} + \frac{ag^2}{2}\sum_{n=1}^{N-1}\underbrace{L_n^2}_{\text{Electric energy}}$$

- Gauss Law: $L_n - L_{n-1} = Q_n = \sum_{f=1}^{F}\left[\phi^\dagger_{n,f}\phi_{n,f} - \frac{1}{2}\left(1-(-1)^n\right)\right]$
- Use open boundary conditions and Gauss Law to integrate out the gauge field

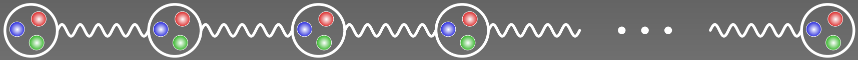

l_0 $\quad Q_1$ $\quad l_1 + Q_2 = l_2$

Multi-flavor Schwinger model

Lattice multi-flavor Schwinger model

- Lattice formulation with Kogut-Susskind staggered fermions

$$H = -\frac{i}{2a}\sum_{n=1}^{N-1}\sum_{f=1}^{F}\left(\phi^{\dagger}_{n,f}\, e^{i\theta_n}\, \phi_{n+1,f} - \text{h.c}\right) + \sum_{n=1}^{N}\sum_{f=1}^{F}\left((-1)^n m_f + \kappa_f\right)\phi^{\dagger}_{n,f}\phi_{n,f} + \frac{ag^2}{2}\sum_{n=1}^{N-1} L_n^2$$

Kinetic part + Coupling to gauge field · Mass term · Chemical potential · Electric energy

- Gauss Law: $L_n - L_{n-1} = Q_n = \sum_{f=1}^{F}\left[\phi^{\dagger}_{n,f}\phi_{n,f} - \frac{1}{2}\left(1-(-1)^n\right)\right]$
- Use open boundary conditions and Gauss Law to integrate out the gauge field

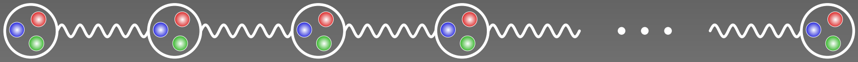

$$l_0 + Q_1 \quad + \quad Q_2 = l_2$$

Multi-flavor Schwinger model

Lattice Hamiltonian formulation

- Applying a residual gauge transformation allows for removing the link operators $e^{i\theta_n}$
- Dimensionless formulation on the gauge invariant subspace

$$W = \frac{2}{ag^2}H = -\boxed{x}\sum_{n=1}^{N-1}\sum_{f=1}^{F}\left(\phi^\dagger_{n,f}\phi_{n+1,f} - \text{h.c.}\right)$$
$$+\sum_{n=1}^{N}\sum_{f=1}^{F}\left((-1)^n\boxed{\mu_f} + \boxed{\nu_f}\right)\phi^\dagger_{n,f}\phi_{n,f} + \sum_{n=1}^{N-1}\left(l_0 + \sum_{k=1}^{n} Q_n\right)^2$$

Multi-flavor Schwinger model

Lattice Hamiltonian formulation

- Applying a residual gauge transformation allows for removing the link operators $e^{i\theta_n}$
- Dimensionless formulation on the gauge invariant subspace

$$W = \frac{2}{ag^2}H = -\boxed{x}\sum_{n=1}^{N-1}\sum_{f=1}^{F}\left(\phi^{\dagger}_{n,f}\phi_{n+1,f} - \text{h.c.}\right) + \sum_{n=1}^{N}\sum_{f=1}^{F}\left((-1)^n\boxed{\mu_f} + \boxed{\nu_f}\right)\phi^{\dagger}_{n,f}\phi_{n,f} + \sum_{n=1}^{N-1}\left(l_0 + \sum_{k=1}^{n} Q_n\right)^2$$

$1/(ag)^2$ $\quad 2m_f/ag^2$ $\quad 2\kappa_f/ag^2$

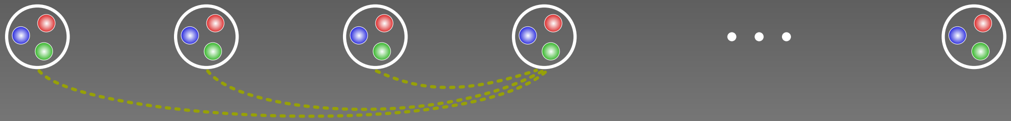

Multi-flavor Schwinger model

Zero temperature phase structure

- Analytical/numerical results are available for $F = 2, 3$
- Phases are characterized by $\Delta N_f = \sum_n \left(\phi^\dagger_{n,f}\phi_{n,f} - \phi^\dagger_{n,k}\phi_{n,k}\right)$, $f \neq k$
- Phases with different ΔN_f first-order phase transitions
- **Sign problem** for Monte Carlo simulations if $\sum_f \nu_f \neq 0$

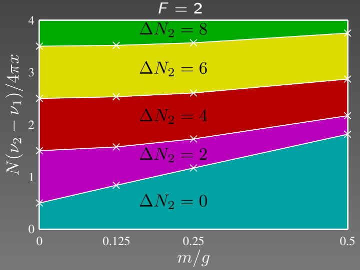

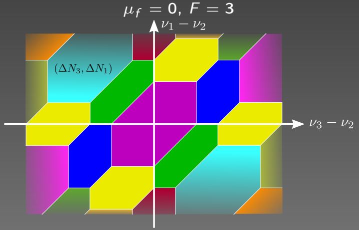

R. Narayanan, Phys. Rev. D , **86**, 125008 (2012)
R. Lohmayer,R. Narayanan, Phys. Rev. D **88**, 105030 (2013)
M.C. Bañuls et al., Phys. Rev. Lett. **118**, 071601 (2017)

2.

Variational Quantum Eigensolver

Variational Quantum Eigensolver (VQE)

- Hybrid quantum-classical algorithm for finding ground states of Hamiltonians W
- Define the cost function to be minimized

$$\mathcal{C}(\vec{\theta}) = \langle \psi(\vec{\theta}) | W | \psi(\vec{\theta}) \rangle$$

A. Peruzzo et al., Nat. Commun. 5, 1 (2014)
J. R. McClean et al., New J. Phys. 18, 023023 (2016)

Variational Quantum Eigensolver

Variational Quantum Eigensolver (VQE)

- Hybrid quantum-classical algorithm for finding ground states of Hamiltonians W
- Define the cost function to be minimized

$$\mathcal{C}(\vec{\theta}) = \langle \psi(\vec{\theta}) | W | \psi(\vec{\theta}) \rangle$$

- Realize a parametric ansatz $|\psi(\vec{\theta})\rangle$ by a parametric quantum circuit

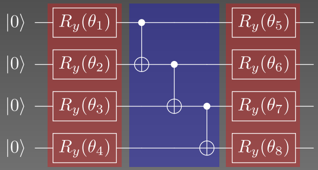

A. Peruzzo et al., Nat. Commun. 5, 1 (2014)
J. R. McClean et al., New J. Phys. 18, 023023 (2016)

Variational Quantum Eigensolver

Variational Quantum Eigensolver (VQE)

- Hybrid quantum-classical algorithm for finding ground states of Hamiltonians W
- Define the cost function to be minimized

$$\mathcal{C}(\vec{\theta}) = \langle \psi(\vec{\theta}) | W | \psi(\vec{\theta}) \rangle$$

- Realize a parametric ansatz $|\psi(\vec{\theta})\rangle$ by a parametric quantum circuit
- Measure the cost function $\mathcal{C}(\vec{\theta})$ on the quantum device

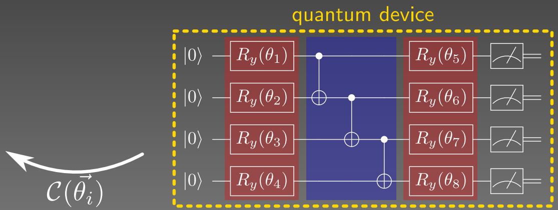

A. Peruzzo et al., Nat. Commun. 5, 1 (2014)
J. R. McClean et al., New J. Phys. 18, 023023 (2016)

Variational Quantum Eigensolver

Variational Quantum Eigensolver (VQE)

- Hybrid quantum-classical algorithm for finding ground states of Hamiltonians W
- Define the cost function to be minimized

$$\mathcal{C}(\vec{\theta}) = \langle \psi(\vec{\theta}) | W | \psi(\vec{\theta}) \rangle$$

- Realize a parametric ansatz $|\psi(\vec{\theta})\rangle$ by a parametric quantum circuit
- Measure the cost function $\mathcal{C}(\vec{\theta})$ on the quantum device
- Optimize the parameters classically to minimize $\mathcal{C}(\vec{\theta})$

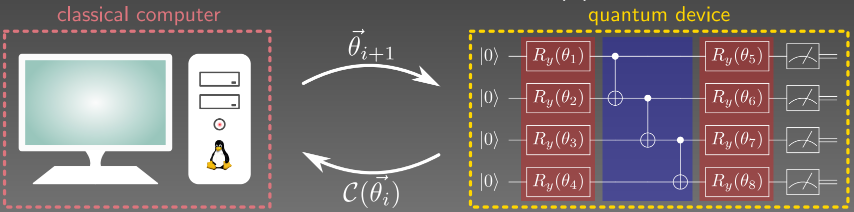

A. Peruzzo et al., Nat. Commun. 5, 1 (2014)
J. R. McClean et al., New J. Phys. 18, 023023 (2016)

Variational Quantum Eigensolver

VQE approach for the Schwinger model with 3 fermion flavors

- Translate the fermions to spins using a Jordan-Wigner transformation
  $\Rightarrow$ Spin Hamiltonian with long-range interactions

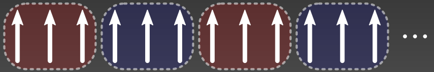

- Incorporate the symmetries of the model
  - Conservation of the total charge $\sum_n Q_n$
  - For antisymmetric chemical potentials $\nu_1 = -\nu_3, \nu_2 = 0$:
    flipping all spins and reflecting around the center of the system

Variational Quantum Eigensolver

Ansatz suitable for the Schwinger model with 3 flavors of fermions

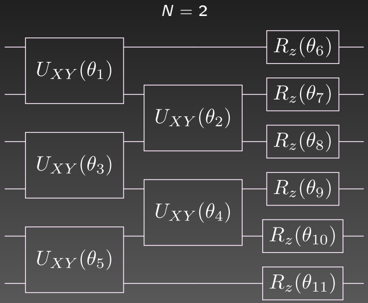

Variational Quantum Eigensolver

Ansatz suitable for the Schwinger model with 3 flavors of fermions

- Use a layered structure consisting of
  - Entangling gates
    $U_{XY}(\theta) = \exp\left(-i\frac{\theta}{2}(XX + YY)\right)$
  - Single-qubit rotations $R_Z(\theta) = \exp\left(-i\frac{\theta}{2}Z\right)$

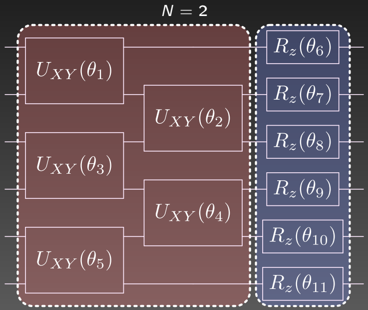

Variational Quantum Eigensolver

Ansatz suitable for the Schwinger model with 3 flavors of fermions

- Use a layered structure consisting of
  - Entangling gates $U_{XY}(\theta) = \exp\left(-i\frac{\theta}{2}(XX + YY)\right)$
  - Single-qubit rotations $R_Z(\theta) = \exp\left(-i\frac{\theta}{2}Z\right)$
- Enforcing the symmetries for $\nu_1 = -\nu_3$, $\nu_2 = 0$: special choice of parameters within one layer
  - Entangling gates: $\theta_k = \theta_{3N-k}$, $k = 1, \ldots, N/2 - 1$
  - Single-qubit rotations: $\theta_k = -\theta_{3N-k+1}$, $k = 1, \ldots, N/2 - 1$

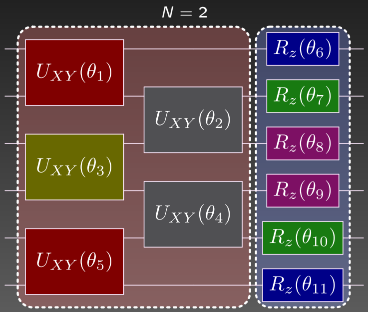

Variational Quantum Eigensolver

Ansatz suitable for the Schwinger model with 3 flavors of fermions

- Use a layered structure consisting of
  - Entangling gates $U_{XY}(\theta) = \exp\left(-i\frac{\theta}{2}(XX + YY)\right)$
  - Single-qubit rotations $R_Z(\theta) = \exp\left(-i\frac{\theta}{2}Z\right)$
- Enforcing the symmetries for $\nu_1 = -\nu_3$, $\nu_2 = 0$: special choice of parameters within one layer
  - Entangling gates: $\theta_k = \theta_{3N-k}$, $k = 1, ..., N/2 - 1$
  - Single-qubit rotations: $\theta_k = -\theta_{3N-k+1}$, $k = 1, ..., N/2 - 1$
- For the general case we choose all parameters independently

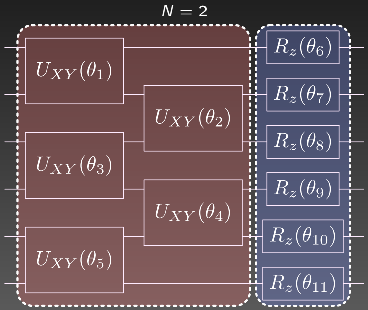

Variational Quantum Eigensolver

Ansatz suitable for the Schwinger model with 3 flavors of fermions

- Use a layered structure consisting of
  - Entangling gates $U_{XY}(\theta) = \exp\left(-i\frac{\theta}{2}(XX+YY)\right)$
  - Single-qubit rotations $R_Z(\theta) = \exp\left(-i\frac{\theta}{2}Z\right)$
- Enforcing the symmetries for $\nu_1 = -\nu_3$, $\nu_2 = 0$: special choice of parameters within one layer
  - Entangling gates: $\theta_k = \theta_{3N-k}$, $k = 1, ..., N/2-1$
  - Single-qubit rotations: $\theta_k = -\theta_{3N-k+1}$, $k = 1, ..., N/2-1$
- For the general case we choose all parameters independently
- Initial state: Neel state for the sites

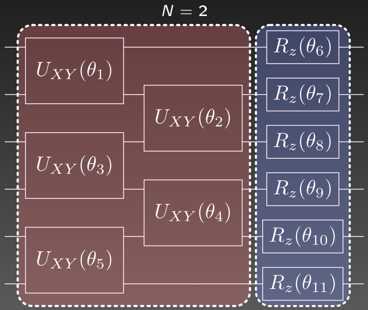

$$|\psi_0\rangle = |111\rangle \otimes |000\rangle \otimes |111\rangle \otimes |000\rangle \ldots$$

3.

Preliminary results

Classical simulation of the VQE

- Simulate the VQE classically for $N = 2, 4, 6$ corresponding to $6, 12, 18$ qubits
- Assume a perfect quantum computer (no errors, no shot noise)
- Use up to 5 layers of the ansatz

Preliminary results

Classical simulation of the VQE

- Simulate the VQE classically for $N = 2, 4, 6$ corresponding to $6, 12, 18$ qubits
- Assume a perfect quantum computer (no errors, no shot noise)
- Use up to 5 layers of the ansatz
- Explore various regimes to see if the ansatz allows for capturing the physics
  1. Antisymmetric case for vanishing mass: $\nu_1 = -\nu_3$, $\nu_2 = 0$, $\mu_f = 0$
     $\Rightarrow$ Analytical results available
  2. Antisymmetric case for nonvanishing mass: $\nu_1 = -\nu_3$, $\nu_2 = 0$, $\mu_f \neq 0$
     $\Rightarrow$ Accessible with Monte Carlo methods
  3. Nonvanishing sum of chemical potentials: $\nu_1 + \nu_2 + \nu_3 \neq 0$
     $\Rightarrow$ Sign problem for Monte Carlo methods

Classical simulation for vanishing bare fermion mass and $\nu_1 = -\nu_3$, $\nu_2 = 0$

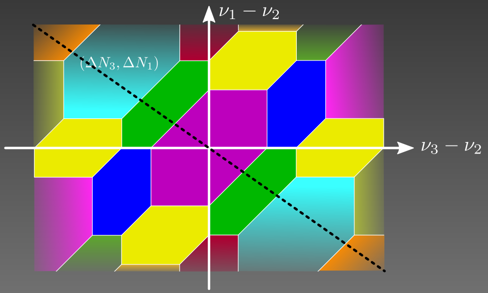

Preliminary results

Classical simulation of the VQE for $x = 16$ and vanishing bare fermion mass $\mu_f = 0$

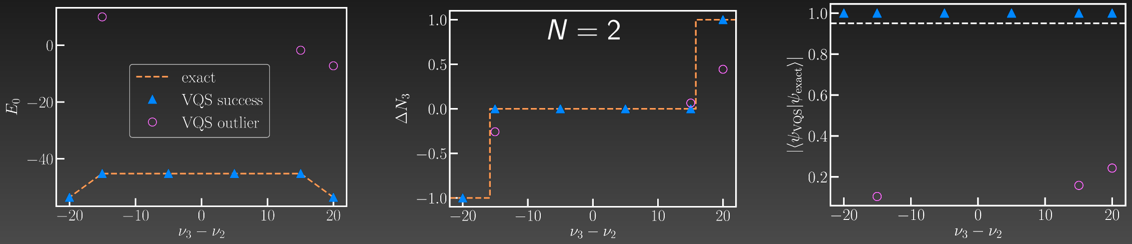

Preliminary results

Classical simulation of the VQE for $x = 16$ and vanishing bare fermion mass $\mu_f = 0$

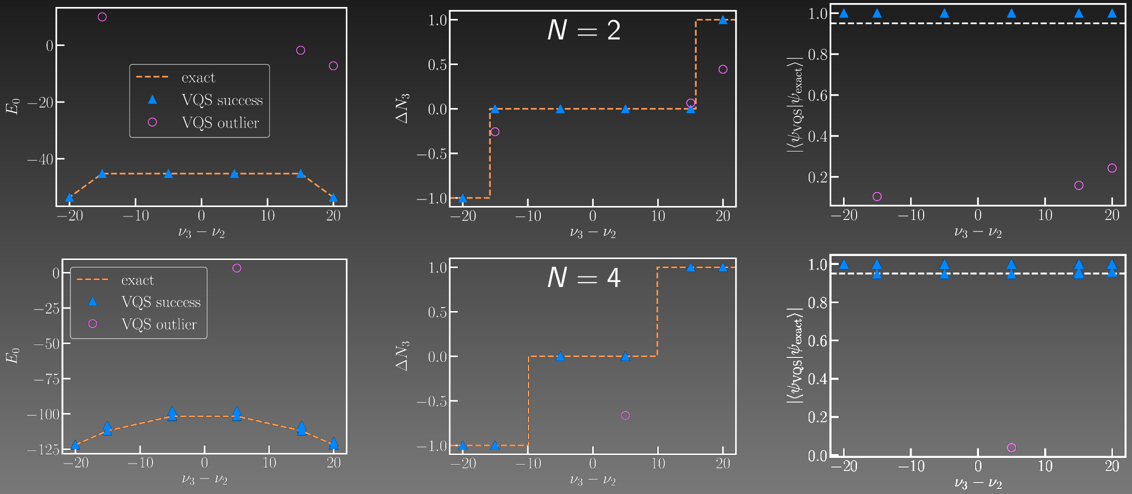

Preliminary results

Classical simulation of the VQE for $x = 16$ and vanishing bare fermion mass $\mu_f = 0$

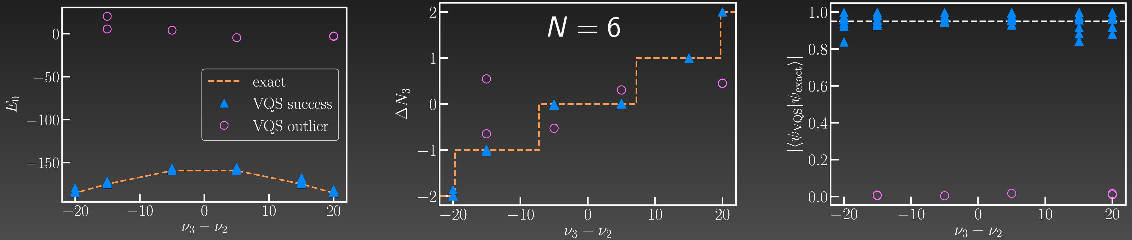

Preliminary results

Classical simulation of the VQE for $x = 16$ and vanishing bare fermion mass $\mu_f = 0$

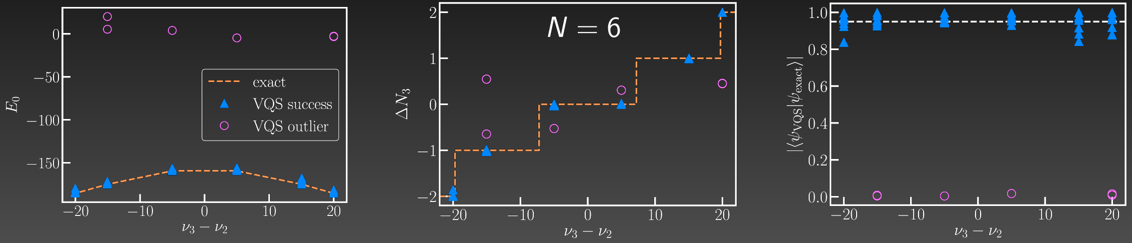

- Good agreement of the VQS results with the exact solution for most cases
- VQS wave function has high overlap with the exact one for most cases
- Characteristic discontinuities in ΔN_3 indicate the first-order phase transitions
- Outliers can be well identified by the experimentally accessible observables energy and ΔN_3 values

Classical simulation for $\mu_f \neq 0$ and $\nu_1 = -\nu_3$, $\nu_2 = 0$

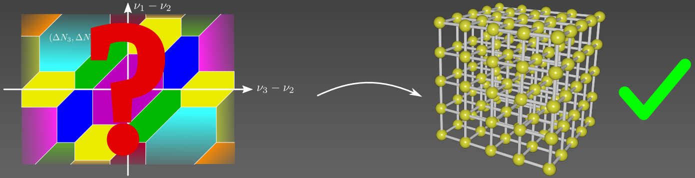

Preliminary results

Classical simulation of the VQE for $x = 16$ and bare fermion mass $\mu_f = 0.8$

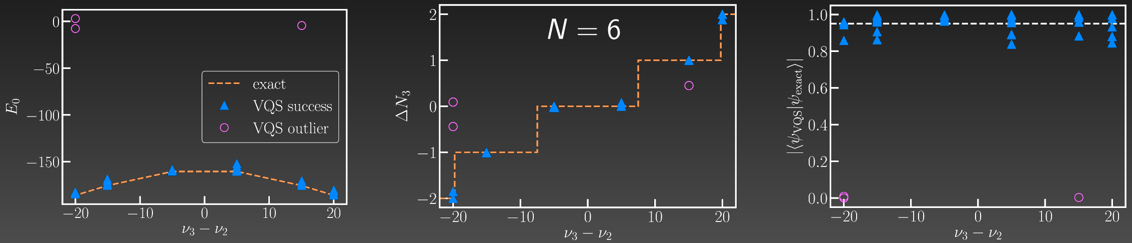

Preliminary results

Classical simulation of the VQE for $x = 16$ and bare fermion mass $\mu_f = 0.8$

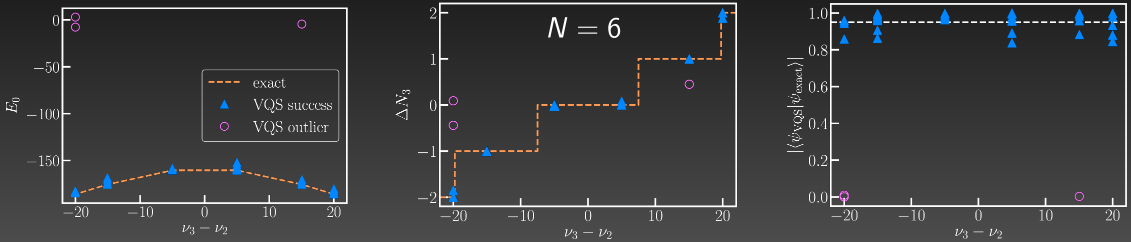

- Similar results as for vanishing bare fermion mass
- Good agreement of the VQS results and high overlap of the VQS wave function with the exact solution for most cases
- Characteristic discontinuities in ΔN_3 indicate the first-order phase transitions
- Outliers can again be well identified by the energy and ΔN_3 values

Classical simulation for $\nu_1 = -\nu_3$, $\nu_2 \neq 0$

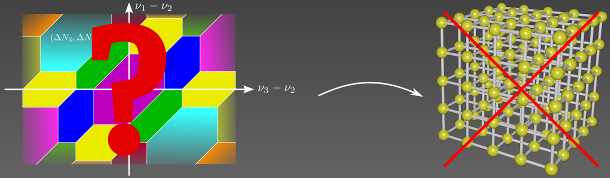

Preliminary results

Classical simulation of the VQE for $x = 16$, vanishing bare fermion mass, and $\nu_2 = 3$

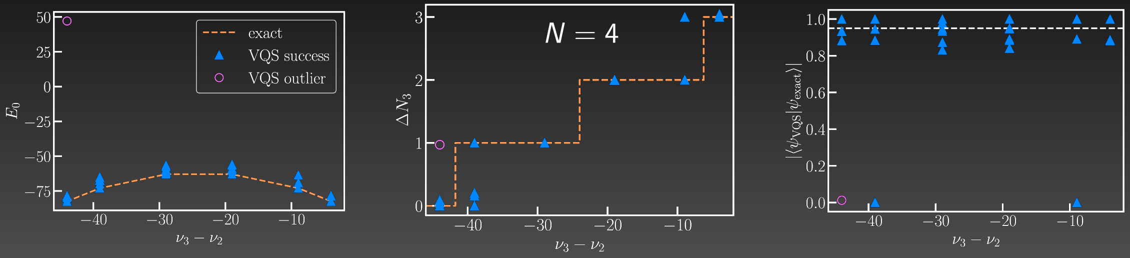

Preliminary results

Classical simulation of the VQE for $x = 16$, vanishing bare fermion mass, and $\nu_2 = 3$

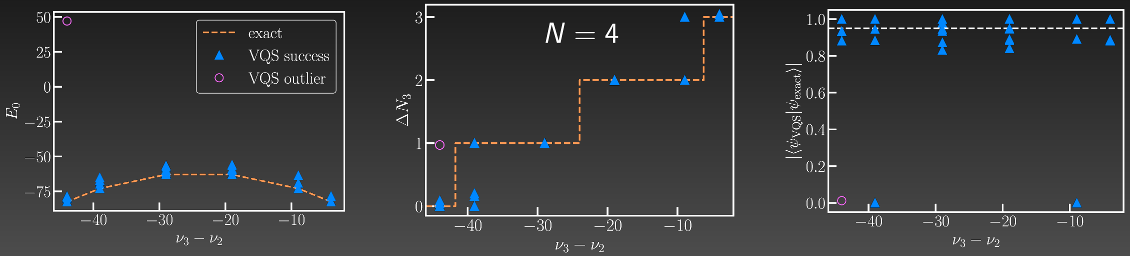

- Ansatz also works for the case $\nu_2 \neq 0$ where the symmetry is no longer present and Monte Carlo encounters a sign problem
- More parameters in the ansatz make the classical optimization more challenging, nevertheless good agreement with exact results
- Some of the outliers might still be improved by running the VQE for a larger number of iterations

Summary & Outlook

Summary

- Ansatz circuit for VQE allows for capturing the relevant physics of the model
- Good results in regimes where Monte Carlo approach suffers from the sign problem
- Classical simulations demonstrate high overlap with exact solution
- Symmetries of the model for antisymmetric choice of the chemical potentials can be easily incorporated in the ansatz to reduce the number of parameters

Summary & Outlook

Summary

- Ansatz circuit for VQE allows for capturing the relevant physics of the model
- Good results in regimes where Monte Carlo approach suffers from the sign problem
- Classical simulations demonstrate high overlap with exact solution
- Symmetries of the model for antisymmetric choice of the chemical potentials can be easily incorporated in the ansatz to reduce the number of parameters

Outlook

- Explore improved optimization techniques
- Study the effects of noise (shot noise, gate errors, measurement errors)
- Implementation on quantum hardware
- Ansatz circuit is suitable for measurement-based quantum computing
  $\Rightarrow$ Opens up the possibility for implementation on alternative platforms

Thank you for your attention!

Questions?

Appendix A. Measurement-based quantum computing

Measurement-based quantum computing

- Equivalent to the circuit model
- Unitary gate operations are implemented via single-qubit measurements
- Based on the single-qubit teleportation protocol

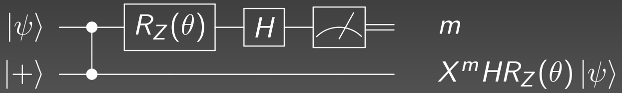

- Measuring the upper qubit in the basis $|\theta_\pm\rangle = R_Z(-\theta)\,|\pm\rangle$ realizes the operation $HR_Z(\theta)\,|\psi\rangle$ in the lower qubit
- Pauli operator is depended on the measurement result and has to be compensated at the end

Appendix A. Measurement-based quantum computing

Measurement-based quantum computing

- Successive application allows for realizing a sequence of single qubit gates

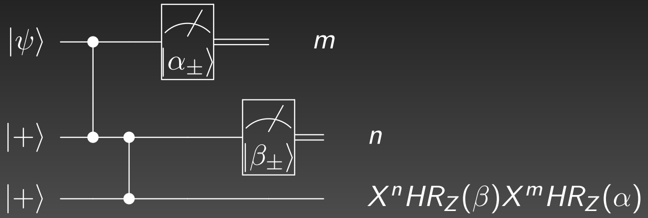

Appendix A. Measurement-based quantum computing

Measurement-based quantum computing

- Successive application allows for realizing a sequence of single qubit gates

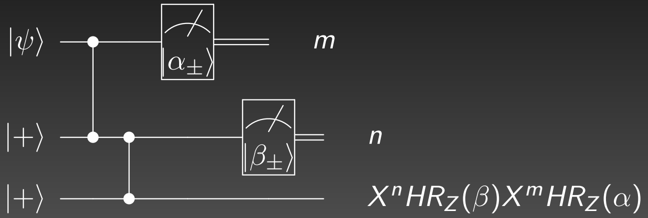

- In order to commute the unwanted Pauli gates to the left an adaptive choice of sign in the next measurement basis is required

$$X^n H R_Z(\beta) X^m H R_Z(\alpha) = \boxed{X^n Z^m} H R_Z((-1)^m \beta) H R^z(\alpha) |\psi\rangle$$

Appendix A. Measurement-based quantum computing

Measurement-based quantum computing

- Successive application allows for realizing a sequence of single qubit gates

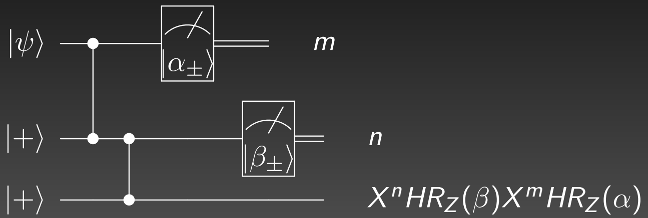

- In order to commute the unwanted Pauli gates to the left an adaptive choice of sign in the next measurement basis is required

$$X^n H R_Z(\beta) X^m H R_Z(\alpha) = \boxed{X^n Z^m} H R_Z((-1)^m \beta) H R^z(\alpha)\,|\psi\rangle$$

- Notation as a graph

Appendix A. Measurement-based quantum computing

Measurement-based quantum computing

- Implementing an algorithm
  1. Rewrite Unitary operations in the gate set $\{R_Z(\theta), H, CZ\}$
  2. Express these unitaries using the teleportation protocol
  3. Create the graph representation

Appendix A. Measurement-based quantum computing

Measurement-based quantum computing

- Implementing an algorithm
  1. Rewrite Unitary operations in the gate set $\{R_Z(\theta), H, CZ\}$
  2. Express these unitaries using the teleportation protocol
  3. Create the graph representation
- Graph representation of a VQE layer for $N = 2$